$(e, 3e)$ observation of the angular correlation between ejected and Auger electrons in the double ionization of magnesium

M. J. Ford and J. P. Doering
Department of Chemistry, Johns Hopkins University, Baltimore, Maryland 21218

M. A. Coplan
Institute for Physical Science and Technology, University of Maryland, College Park, Maryland 20742

J. W. Cooper and J. H. Moore
Department of Chemistry and Biochemistry, University of Maryland, College Park, Maryland 20742
(Received 21 March 1994; revised manuscript received 25 July 1994)

Electron-impact excitation of the $L_{2,3}M_1M_1$ Auger process in magnesium has been observed in a triple-coincidence experiment. A 3.5-keV incident electron is used and the scattered electron, the ejected $2p$ electron, and the 35-eV Auger electron are detected. The experiment was performed for ejected electron energies of 35, 45, and 100 eV. Three-dimensional angular distributions for the ejected and Auger electrons were recorded for a fixed scattered-electron direction. A model is presented which describes the angular distribution by additive terms representing the anisotropy in the distribution of ejected and Auger electrons relative to the momentum transfer direction, and the angular correlation between the ejected and Auger electrons. Three corresponding parameters are extracted from the data and compared with the results of a calculation based on a two-step model of ionization and Auger emission.

PACS number(s): 32.80.Hd

INTRODUCTION

When inner-shell vacancies are created in a randomly oriented sample of atoms or molecules as a result of ionization by a beam of electrons or photons, the decay products, Auger electrons, or fluorescent radiation will, in general, be polarized and have an anisotropic angular distribution about the axis of the incident beam [1]. The reason for this is that the angular momentum vector of the decaying ion will be aligned relative to the incident beam direction if angular momentum is transferred to the ion in the initial ionization process. Furthermore, if the ejected electron is detected in coincidence with an Auger electron, the fragmentation pattern for ejected and Auger electrons becomes more complicated since the doubly charged ion has, in addition to its alignment relative to the incident beam direction, an alignment with respect to the ejected-electron direction. It follows that there will be an angular correlation between the Auger and ejected electrons [2].

The effect of core alignment on the angular distribution and polarization of products following the creation of a core hole has been demonstrated for both photoionization and electron-impact ionization. In the photoionization experiments, angular distributions of photoelectrons and Auger electrons [3] as well as fluorescent photons [4] have been measured. The polarization of emitted electrons [5] and photons [4] have also been recorded. For electron-impact ionization, there have been experiments in which the scattered electron was detected in coincidence with ejected or Auger electrons [6–8]. Recently, Kammerling and Schmidt reported the observation of the angular correlation between Auger and ejected electrons in an experiment where Auger electrons from xenon were detected in coincidence with photoelectrons following the creation of a $4d$ hole by 94.5-eV linearly polarized radiation [9]. Here we report the observation of the angular correlation between ejected and Auger electrons following electron-impact ionization. The scattered, ejected, and Auger electrons are detected in triple coincidence—an $(e,3e)$ experiment.

We have investigated the Mg $L_{2,3}M_1M_1$ Auger process, which proceeds by the electron-impact ejection of a $2p$ electron and the emission of the Auger electron with 35-eV energy. A beam of 3.5-keV electrons is crossed with a jet of magnesium atoms. Inelastically scattered electrons are detected within a small solid angle in the forward direction in order to select events with small momentum transfer. Two secondary electrons are detected at angles between 45° and 135° with respect to the incident electron direction, one with 35-eV energy, the energy of the Auger electron, and one with an energy of either 100, 45, or 35 eV. The energy lost by the inelastically scattered incident electron is chosen in each case to correspond to a final state of the system, which consists of two secondary electrons of the specified energy and a doubly charged magnesium ion in the ground state. The coincident detection of three electrons, a scattered and two secondary electrons, assures that all three originated in the same event. The choice of energies assures that the event corresponds to the Auger process since the direct ejection of two $3s$ electrons is much less probable than the resonant Auger process. The independent variables, illustrated in Fig. 1, are θ_1 and θ_2, the angles between each secondary-electron trajectory and the incident electron direction, and θ_{12}, the included angle between the

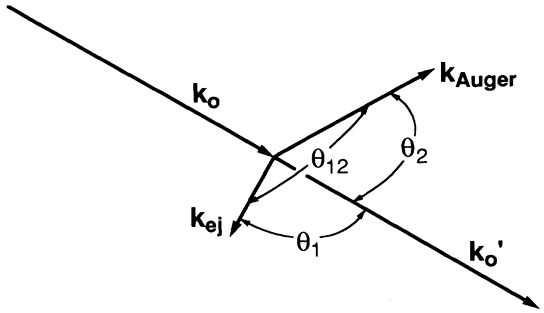

FIG. 1. The geometry of the experiment in terms of the momenta of the incident electron ($\mathbf{k}_0$), the scattered electron ($\mathbf{k}_0'$), the ejected electron ($\mathbf{k}_{ej}$), and the Auger electron ($\mathbf{k}_{Auger}$): θ_1 defines the direction of an ejected electron relative to the direction of the forward-scattered incident electron, θ_2 is the angle between the Auger and scattered electron directions, and θ_{12} is the angle between the ejected and Auger electrons.

two secondaries. When the two secondary-electron energies are unequal, the 35-eV electron can be identified as the Auger electron and the other secondary as the ejected $2p$. In this case, θ_1 is taken to be the angle of the ejected electron and θ_2 the angle of the Auger.

EXPERIMENT

A schematic diagram of the apparatus is shown in Fig. 2. Electrons from a cathode-ray-tube type electron gun intersect, at a right angle, a jet of magnesium atoms emanating from the oven. Scattered incident electrons falling within a solid angle of 2.0×10^{-4} sr in the forward direction are decelerated by a factor of about 17 and those of the desired energy are selected with a hemispherical electrostatic analyzer (the "primary electron analyzer"; the decelerating lens system is not shown in the schematic). Transmitted electrons are detected with an Optotechnik KBL 408 electron multiplier. Secondary electrons of the desired energy are selected with a pair of doubly truncated spherical electrostatic analyzers (the "secondary-electron analyzers") located on opposite sides of the scattering volume on an axis perpendicular to the incident electron direction. An array of four Optotechnik electron multipliers on the output of each of these analyzers detect secondaries of the desired energy. The position of each detector defines the angle of emission of the detected electron within a solid angle of acceptance of 0.04 sr. The energy resolution of each of the three analyzers is about 4 eV. The joint resolution for the detection of three electrons is sufficient to discriminate the ground state of the ion from all excited states, but not sufficient to distinguish between the two components of the 35-eV Auger doublet (34.86 and 35.13 eV). When one of the ejected-electron analyzers is set to transmit 45-eV electrons, several satellite Auger lines near 45 eV present a potential interference, but they are sufficiently weak (6% of the $L_{2,3}M_1M_1$ Auger doublet [10]) as to be unimportant in the present analysis. The angle and energy resolution in these experiments assures that the momentum transfer in the Auger excitation process does not exceed 0.29 a.u.

The events of interest give rise to the arrival of three electrons, correlated in time, one at the primary analyzer detector and two at secondary analyzer detectors. When the secondary analyzers are set to transmit different energies, an $(e,3e)$ event can be observed with the primary detector and one detector on each of the secondary analyzers. For equal energy secondary electrons, an $(e,3e)$ event may give a signal at two of the detectors on one of the secondary analyzers. With the arrangement of detectors shown in Fig. 2, $(e,3e)$ events can be observed

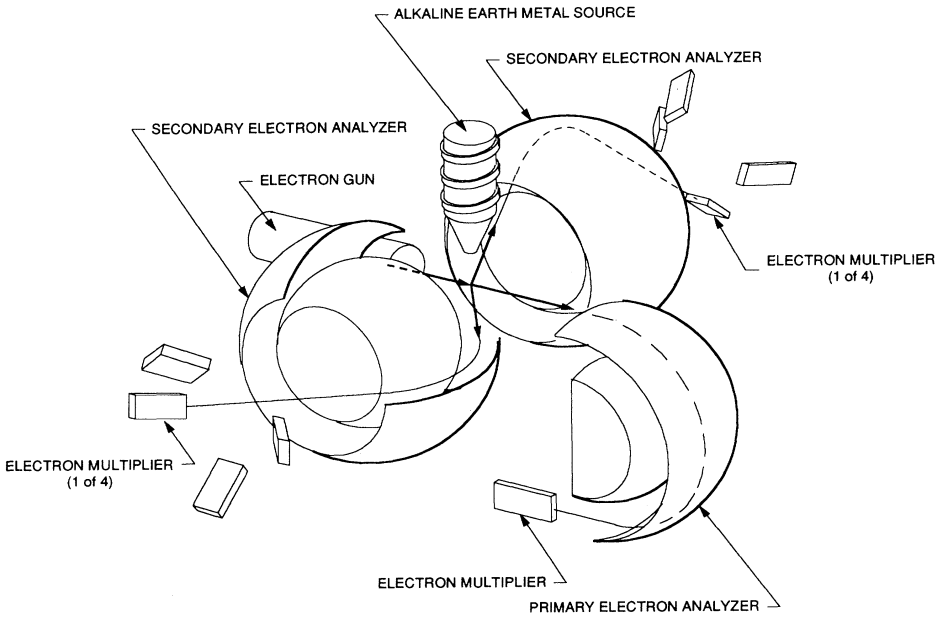

FIG. 2. Schematic illustration of the apparatus. A detected $(e,3e)$ event gives rise to a signal at the primary analyzer electron multiplier and two of the secondary analyzer electron multipliers.

with θ_1 or θ_2 equal to 45°, 60°, 90°, or 135°. For unequal secondary-electron energies, the possible values of θ_{12} are 90°, 98°, 120°, 149°, and 180°. For equal secondary-electron energies, the possible values of θ_{12} are 31°, 60°, 82°, 90°, 98°, 120°, 149°, and 180°.

An $(e,3e)$ event does not give three truly coincident signals owing to differences in flight times and electronic processing times for each of the three electrons, rather the three signals arrive with a fixed time correlation. The rate of arrival of a pair of pulses, one from the primary analyzer and one from one of the secondary detectors is recorded as a function of arrival-time difference over a range of 200 ns. Similarly the rate of arrival as a function of time difference is recorded for the primary detector and another of the secondary detectors. These data are stored as a three-dimensional array, an $(e,3e)$ time spectrum. An example is shown in Fig. 3. The x and y axes give the two time differences and the z axis the corresponding rate. The true, time-correlated $(e,3e)$ events appear as a peak in the middle of the time spectrum. Other important features include (i) a uniform background caused by the random, accidental arrival of three uncorrelated electrons within the time interval covered by the spectrum and (ii) "walls", which are the result of a pair of electrons originating from the same event [an $(e,2e)$ event] in accidental coincidence with a third electron from some random event. There are three such walls that arise from two-electron events, which produce a signal at each of the secondary detectors, or at the primary detector and one of the secondary detectors, or at the primary and the other secondary detector. The amplitude of the uncorrelated accidental background and the amplitude of each of the walls under the central peak must be subtracted from the peak amplitude to give the rate of true $(e,3e)$ events. The rate of $(e,3e)$ events for the primary detector in combination with two of the secondary detectors is a measure of the differential Auger emission cross section for the corresponding values of θ_1, θ_2, and θ_{12}.

Our multidetector apparatus permits us to make many $(e,3e)$ measurements simultaneously. With the secondary analyzers set at different energies this arrangement allows for the simultaneous performance of 16 $(e,3e)$ measurements corresponding to all combinations of the scattered electron detector with an ejected-electron detector and an Auger detector. With both secondary analyzers set to the same energy, 28 measurements are carried out. In fact, the orientation of detectors is such that certain sets of independent variables $(\theta_1,\theta_2,\theta_{12})$ are sampled by more than one combination of detectors. This reduces the size of the $(e,3e)$ data set but provides an important check on the symmetry of the apparatus. Run-to-run variations in the results were within the statistical uncertainty of the data. A small correction was applied to account for a systematic variation in sensitivity associated with the orientation of the rectangular multiplier apertures relative to the beam direction; otherwise, no corrections were necessary.

RESULTS AND DISCUSSION

Equal-energy secondary electrons

Analysis of the data is complicated by the fact that the cross section is measured as a function of three angular variables; however, for equal-energy, 35 eV, secondary

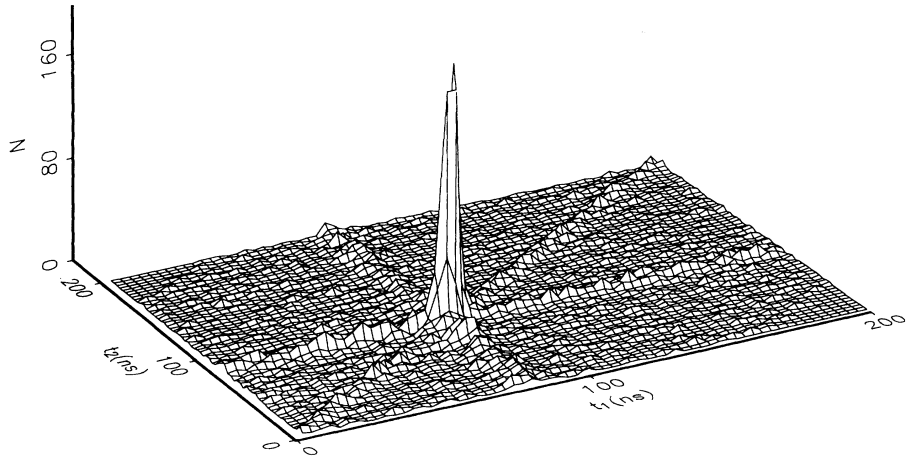

FIG. 3. $(e,3e)$ time spectrum recording the number of occurrences of a primary electron signal and two secondary electron signals within an interval of 200 ns. One horizontal axis corresponds to the time difference τ_1 between the arrival of a primary electron and one of the secondaries, and the other horizontal axis gives the time difference τ_2 between the primary and the other secondary electron. The spectrum was recorded over a period of 20 h with an incident current of about 1 μA and a target density of approximately 10^{13} cm^{-3}

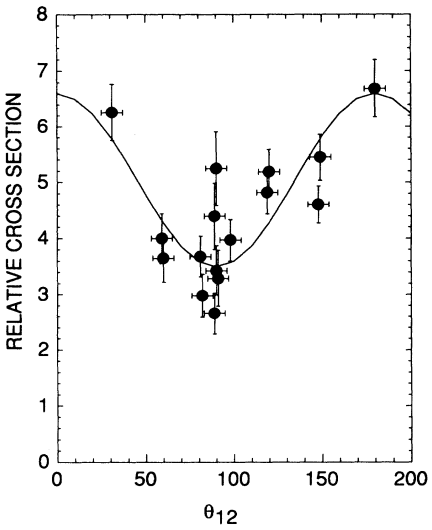

FIG. 4. The relative cross section for the emission of two 35-eV secondary electrons as a function of θ_{12}, the included angle in degrees between the direction of the two electrons. The data are plotted without regard for the direction of either secondary electron with respect to the direction of the forward-scattered incident electron.

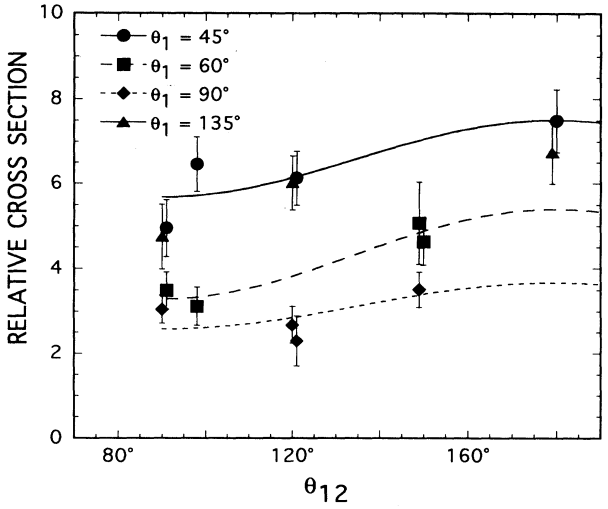

FIG. 5. The relative cross section for the ejection of a 45-eV electron and the emission of a 35-eV Auger electron as a function of θ_{12}, the included angle between the direction of the two electrons. The data are identified according to θ_1, the angle between the directions of the ejected electron, and the forward-scattered incident electron.

electrons, where Auger and ejected electrons cannot be distinguished from one another, the measured relative cross section appears to be a strong function only of the included angle θ_{12}. This is evident in Fig. 4 where the data are plotted as a function of θ_{12} without regard for the direction of either secondary electron with respect to the incident electron direction. The solid curve in Fig. 4 is only to guide the eye, although for consistency with the analysis given below, the form of this curve was chosen to be a linear function of $\cos^2\theta_{12}$. It is important to note that the cross section is large for both small (30°) and large (180°) values of θ_{12} and tends to be small near 90°. This implies that Coulombic repulsion between the two secondaries is not an important factor in the relative angular distribution of the low-energy electrons.

Unequal-energy secondary electrons

The situation is more complex for unequal secondary-electron energies where the ejected and Auger electrons can be distinguished from one another. The angular distribution of secondaries is then a function of more than one of the angular variables. This can be seen in Fig. 5, where the data for 45-eV ejected electrons are plotted as a function of θ_{12}. Although there is a dependence on θ_{12}, it can be seen that the data are segregated according to the value of θ_1, the angle of the ejected electron relative to the incident direction. The cross section is large for ejection in the forward ($\theta_1=45°$) or backward ($\theta_1=135°$) directions and small for ejection at right angles to the incident direction ($\theta_1=90°$). This implies an angular distribution of ejected electrons similar to what would be observed in the photoionization of a $2p$ electron [11]. Accordingly, we have chosen to describe our $(e,3e)$ observations of the joint angular distribution of ejected and Auger electrons in terms similar to the formalism developed by Kabachnik [12] to describe an equivalent photoionization experiment, such as was carried out by Kammerling and Schmidt [9]. This is justified since electron-impact ionization is equivalent to photoionization if the momentum transfer in electron-impact ionization is sufficiently small and in the forward direction.

A model

Assuming a two-step Auger process within an independent-particle model, Schmidt [13], with reference to Kabachnik, has given the following expression for the joint angular distribution of Auger and photoelectrons for the ejection of a $2p_{3/2}$ electron from magnesium:

$$\frac{d^2\sigma}{d\Omega_1 d\Omega_2}=\frac{\sigma_t}{4\pi}[1+\beta_1 P_2(\cos\theta_1)+\beta_2 P_2(\cos\theta_2) +F(\theta_1,\phi_1,\theta_2,\phi_2)]\,, \quad (1)$$

where θ_1 and θ_2 define the directions of the photoelectron and Auger electron, respectively, relative to the axis of polarization and Ω_1 and Ω_2 are the corresponding solid angles over which electrons are detected, σ_t is the total cross section for $2p_{3/2}$ ionization, β_1 and β_2 are, respectively, the parameters describing the degree of anisotropy in the angular distribution of photoelectrons and Auger electrons in a noncoincident experiment, $P_2(\cos\theta)$ refers to the second Legendre polynomial, and the last term describes the angular correlation between photo- and Auger electrons. For $2p_{1/2}$ ionization, the expression is the same with β_2 and F identically zero. An analysis of the formalism of Ref. [12] revealed that the last term of Eq.

(1) can be approximated to within a few percent by a term proportional to $P_2(\cos\theta_{12})$, thus suggesting the following expression to model the joint angular distribution measured in our experiment:

$$\frac{d^2\sigma}{d\Omega_1 d\Omega_2}=\frac{\sigma_t}{4\pi}[1+\beta_1 P_2(\cos\theta_1)+\beta_2 P_2(\cos\theta_2) +\beta_{12}P_2(\cos\theta_{12})] , \quad (2)$$

where β_{12} describes the anisotropy in the relative angular distribution of the ionized electron and the Auger electron. β_{12} is a measure of the extent of the correlation between the ionized electron and the Auger electron. As discussed in Refs. [11] and [13], the parameters β_1 and β_2 depend only upon two dipole matrix elements and the phase difference between s and d waves. Within the two-step independent particle model of Ref. [12], β_{12} also depends only on these parameters and is simply equal to $\beta_1/3$.

For each set of energy conditions, a multiple linear regression analysis was employed to fit the data to the form of the bracketed expression on the right side of Eq. (2). The values of the β parameters thus obtained are given in Table I along with the statistical uncertainty (related to that in the data) and the multiple-correlation coefficient R (as a measure of the quality of fit) [14].

For comparison with experiment, β parameters were calculated using the formulas given in Ref. [12]. Values for β_1 and β_2 were obtained from a Herman-Skillman (*H-S*) central-potential calculation [15,16]. An additional set of values for β_1 were obtained from a calculation employing the relativistic random-phase approximation (RRPA) [17]. Account must be taken of the fact that the experiment does not distinguish between $2p_{3/2}$ and $2p_{1/2}$ ionization; hence the results of the calculations reported in Table I are the appropriately weighted average of the β parameters for the two cases.

As shown in Table I the values of the parameters obtained in fitting the data to Eq. (2) are in qualitative agreement with those from the theoretical calculations. The experimental values for β_1 decrease with decreasing ejected-electron energy as predicted, but are somewhat smaller than the theoretical values. This is similar to what was observed in the photoionization experiment of Ref. [11] where β_1 was measured to be 0.74 ± 0.02 for a photon energy of 80 eV and an ejected-electron energy of 26 eV, whereas the Herman-Skillman value at this energy is 0.96. The value of β_2 from the analysis of the data was found to be much smaller than β_1 as predicted theoretically and as observed in the photoionization experiment. The result is the determination of β_{12}, a measure of the angular correlation between the ejected and Auger electrons. Within the precision of the experiment $\beta_{12}=\beta_1/3$, as obtained from theory.

TABLE I. The anisotropy in the angular distribution of electrons in the Mg $L_{2,3}M_1M_1$ Auger process excited by 3.5-keV electron impact in terms of the model defined by Eq. (2). β_1 describes the anisotropy in the distribution of ejected electrons relative to the incident electron direction; β_2 the anisotropy in the distribution of Auger electrons relative to the incident electron direction; and β_{12} the angular correlation between the Auger electron and the ejected electron. Experimental values (Expt.) obtained from a fit to the measured relative cross sections. Theoretical values are from the Herman-Skillman (HS) and RRPA calculations. The cited uncertainties reflect the statistical uncertainty in the data and R is the multiple-correlation coefficient of the fit of the data to the model.

	β_1	β_2	β_{12}	R
	100-eV ejected electron; 35-eV Auger electron			
Expt.	1.11±0.15	0.07±0.14	0.31±0.09	0.87
HS	1.45	0.09	0.48	
RRPA	1.39		0.46	
	45-eV ejected electron; 35-eV Auger electron			
Expt.	0.85±0.09	−0.26±0.11	0.26±0.06	0.96
HS	1.20	0.09	0.40	
RRPA	1.12		0.37	

SUMMARY

Electron-impact excitation of the $L_{2,3}M_1M_1$ Auger process in magnesium has been investigated in an experiment in which all three product electrons are detected in coincidence. For the case of equal-energy ejected and Auger electrons, we find the cross sections for the process to have a strong dependence on the angle between the direction of these two electrons. A similar result is observed when the kinetic energy of the ejected electron exceeds that of the Auger electron. For the latter cases, a parametrization scheme has been employed to compare the results of the experiment with a calculation based on a two-step model of ionization and Auger emission.

ACKNOWLEDGMENTS

This work was supported by the National Science Foundation, Grant No. PHY-91-07337. Additional support was provided by NATO collaborative Research Grant No. CRG 920101 and by the University of Maryland (J.H.M.).

[1] E. G. Berezhko and N. K. Kabachnik, J. Phys. B **10**, 2467 (1977).
[2] E. G. Berezhko and N. K. Kabachnik, J. Phys. B **12**, 2993 (1979).
[3] S. Southworth, U. Becker, C. M. Truesdale, P. H. Kobrin, D. W. Lindle, S. Owaki, and D. A. Shirley, Phys. Rev. A **28**, 261 (1983).
[4] H. Klar J. Phys. B **13**, 2037 (1980), and references therein.
[5] U. Heinzmann, in Proceedings of the International Conference on Vacuum Ultraviolet Radiation Physics

Lund, 1987, edited by P. O. Nilson and J. Nordgren, [Phys. Scr. **T17**, (1987)], and references therein.
[6] W. Sandner and M. Volkel, J. Phys. B **17**, L597 (1984).
[7] E. C. Sewell and A. Crowe, J. Phys. B **17**, 2913 (1984).
[8] G. Stefani, L. Avaldi, A. Lahmam-Bennani, and A. Duguet, J. Phys. B **19**, 3787 (1986).
[9] B. Kammerling and V. Schmidt, Phys. Rev. Lett. **67**, 1848 (1991).
[10] B. Breuckmann, V. Schmidt, and W. Schmitz, J. Phys. B **9**, 3037 (1976); V. Pejcev, T. W. Ottley, D. Rassi, and K. J. Ross, J. Phys. B **10**, 2389 (1977).
[11] A. Hausmann, B. Kammerling, H. Kossmann, and V. Schmidt, Phys. Rev. Lett. **61**, 2669 (1988).
[12] N. M. Kabachnik, J. Phys. B **25**, L369 (1992).
[13] V. Schmidt, in *X-ray and Inner-Shell Processes,* edited by T. A. Carlson, M. O. Krause, and S. T. Manson, AIP Conf. Proc. No. 215 (AIP, New York, 1990), pp. 559–581.
[14] P. R. Bevington, *Data Reduction and Error Analysis for the Physical Sciences* (McGraw-Hill, New York, 1969), pp. 131–132, 198–199.
[15] F. Herman and S. Skillman, *Atomic Structure Calculations* (Prentice-Hall, Englewood Cliffs, NJ, 1963).
[16] S. T. Manson and J. W. Cooper, Phys. Rev. **165**, 165 (1968).
[17] P. C. Desmukh and S. T. Manson, Phys. Rev. A **28**, 209 (1983); S. T. Manson (private communication).